# Sine-Transform-Based Chaotic System With FPGA Implementation

Zhongyun Hua, *Member, IEEE*, Binghang Zhou, and Yicong Zhou, *Senior Member, IEEE*

***Abstract*—As chaotic dynamics is widely used in nonlinear control, synchronization communication, and many other applications, designing chaotic maps with complex chaotic behaviors is attractive. This paper proposes a sine-transform-based chaotic system (STBCS) of generating one-dimensional (1-D) chaotic maps. It performs a sine transform to the combination of the outputs of two existing chaotic maps (seed maps). Users have the flexibility to choose any existing 1-D chaotic maps as seed maps in STBCS to generate a large number of new chaotic maps. The complex chaotic behavior of STBCS is verified using the principle of Lypunov exponent. To show the usability and effectiveness of STBCS, we provide three new chaotic maps as examples. Theoretical analysis shows that these chaotic maps have complex dynamics properties and robust chaos. Performance evaluations demonstrate that they have much larger chaotic ranges, better complexity, and unpredictability, compared with chaotic maps generated by other methods and the corresponding seed maps. Moreover, to show the simplicity of STBCS in hardware implementation, we simulate the three new chaotic maps using the field-programmable gate array (FPGA).**

***Index Terms*—Chaotic behavior, field-programmable gate array (FPGA), nonlinear control, sine-transform-based chaotic system (STBCS).**

## I. Introduction

CHAOTIC behavior, as a kind of dynamical behaviors, was first observed in meteorology to describe the unpredictability of weather [1]. Subsequently, chaos phenomena are found wide existence in many natural and non-natural behaviors, such as road traffic and stock marketing [2], [3]. According to the Devaney's definition, chaotic behaviors show the following properties [4]:

1) Initial condition sensitivity.
2) Topologically mixing.
3) Periodic orbits density.

The initial condition sensitivity means that arbitrarily little difference of the initial conditions eventually leads to totally different behaviors; the topologically mixing demonstrates that any given region of the phase plane can overlap any other given region with the trajectory evolves; the periodic orbits density indicates that the periodic orbits can arbitrarily approach every point of the phase plane. Because these significant properties are quite similar with the principles of many real applications, chaos theory attracts increasing research attentions in various disciplines [5], [6], especially in nonlinear control [7], [8] and cryptography [9], [10].

Chaotic systems are some mathematical equations/models derived from the rules of describing chaotic behaviors. For example, the logistic map is designed to simulate the population growth [11] and the Lorenz system is the mathematical model of describing the atmospheric convection [1]. Theoretically, a chaotic system's chaotic attractors are locally oscillating but globally stable. This demonstrates that arbitrarily approached states will separate from each other but the whole attractors will not depart from the region with the system evolves [12]. However, all the software/hardware platforms cannot own infinite precision. When chaotic systems are simulated in these finite precision platforms, some extremely approached states may overlap, which unavoidably makes chaotic distribution degrade to periodic distribution [13]–[15]. This may cause negative impacts to some chaos-based applications. Recently, many chaos-based applications are identified to have secure problems because of the chaos degradation [16], [17]. On the other hand, as the fast development of discerning chaos technologies and improvement of computer ability, some existing chaotic systems with simple definitions and low complexity can be estimated by identifying their chaotic states [18], [19], estimating their chaotic orbits [20], [21], or deducing the initial states [22], [23]. This also causes bottlenecks for the chaos-based applications [24], [25].

Nowadays, a wide body of researches has been devoted to counteracting the chaos degradation and improving the performance of existing chaotic systems [26]–[28]. These works can

Manuscript received December 31, 2016; revised June 9, 2017; accepted June 25, 2017. Date of publication August 7, 2017; date of current version December 15, 2017. This work was supported in part by the National Natural Science Foundation of China under Grant 61701137, in part by the Shenzhen Science and Technology Innovation Council under Grant JCYJ20170307150704051, in part by the Macau Science and Technology Development Fund under Grant FDCT/016/2015/A1, and in part by the Research Committee at the University of Macau under Grant MYRG2014-00003-FST and Grant MYRG2016-00123-FST. *(Corresponding author: Yicong Zhou.)*

Z. Hua is with the School of Computer Science and Technology, Harbin Institute of Technology Shenzhen Graduate School, Shenzhen 518055, China (e-mail: huazyum@gmail.com).

B. Zhou is with the College of Electrical and Information Engineering, Hunan University, Changsha 410082, China (e-mail: hn_zhoubh@qq.com).

Y. Zhou is with the Department of Computer and Information Science, University of Macau, Macau 999078, China (e-mail: yicongzhou@umac.mo).

Color versions of one or more of the figures in this paper are available online at http://ieeexplore.ieee.org.

Digital Object Identifier 10.1109/TIE.2017.2736515

be divided into two categories: 1) Disturbing the signal of existing chaotic systems using different methods; 2) designing new chaotic systems with better performance. Some examples of the first category are as follows. Li *et al.* proposed a reseeding-mixing method to extend the period length of chaotic systems in [29]. Hu *et al.* developed a changeable parameter compensation method to improve the properties of chaotic systems in [30]. Deng *et al.* brought forward a novel control method based on the differential mean value theorem and state feedback technology, which has robustness and superiority in [31]. Some examples of the second category are as follows. Huang *et al.* designed a multiwing butterfly chaotic attractors by designing piecewise hysteresis functions and using them to take the place of the state variables of the Lorenz system [32]. Shen *et al.* developed a systematic methodology to construct continuous-time hyperchaotic systems with complex chaotic behaviors [33].

Compared with the technologies of disturbing the signal of existing chaotic systems, the efforts of generating new chaotic systems can better promote the chaos-based practical applications. However, these works also have some limitations. Specifically, some of new chaotic systems cannot obtain good enough chaos performance and some of them cannot have robust chaos [34]. The robust chaos means the absence of periodic windows and coexisting attractors in some neighborhood of the parameter space [35]. A chaotic system with robust chaos has stable chaos property and can avoid the chaos degradation caused by parameter perturbation in practical applications [36]. Many efforts have proved that chaotic systems with robust chaos can show high efficiency in different practical applications [37]–[39]. In [40], Wu *et al.* proposed a wheel-switching system that can use existing chaotic maps to obtain new ones. But the generated new chaotic maps have limited chaos performance and cannot obtain robust chaos. In [41], Hua and Zhou introduced a parameter-control chaotic system to generate new chaotic maps. Some of the generated chaotic maps have robust chaos and some of them have frail chaos performance. In [42], Zhou *et al.* proposed a new one-dimensional (1-D) chaotic systems that can generate new chaotic maps with robust chaos. But the properties of new chaotic maps may not be theoretically analyzed because a modular operation is contained.

To generate new chaotic maps with robust chaos and extremely good chaos performance, this paper proposes a sine-transform-based chaotic system (STBCS) as a general framework of 1-D chaotic maps. It first combines the outputs of two existing chaotic maps (seed maps) together, and then does the sine transform to the combination result to obtain the final output. Any existing 1-D chaotic maps can be used as the seed maps in STBCS to generate a large number of new chaotic maps. Theoretical analysis and experimental results demonstrate the excellent chaos performance of STBCS. The main novelties and contributions of this paper are summarized as follows.

1) We propose STBCS as a general framework that can use any two existing 1-D chaotic maps as seed maps to generate a large number of new chaotic maps.
2) We discuss the properties of STBCS and investigate its chaotic behavior.
3) To demonstrate the effectiveness of STBCS, we generate three new chaotic maps using STBCS and analyze their dynamics properties.
4) We quantitatively evaluate the performance of the new chaotic maps generated by STBCS, and compare these new chaotic maps with chaotic maps generated by two other methods and the corresponding seed maps.
5) We further implement the three new chaotic maps using field-programmable gate array (FPGA) in hardware platforms.

TABLE I
DESCRIPTIONS OF IMPORTANT NOTATIONS

| Notation | Description |
|---|---|
| $x_i$ | The input/output of a dynamical system |
| $\mathcal{L}(x_i)$ | The logistic map |
| $\mathcal{S}(x_i)$ | The sine map |
| $\mathcal{T}(x_i)$ | The tent map |
| $\mathcal{N}(x_i)$ | The proposed STBCS |
| $\lambda$ | The Lyapunov exponent |
| $\mathcal{H}(x_i)$ | The combination of seed maps of STBCS |
| $\tilde{\mathcal{S}}(x)$ | The sine map with control parameter $r = 1$ |
| $\mathbf{J}$ | The Jacobian matrix |

The rest of this paper is organized as follows. Section II reviews three existing 1-D chaotic maps. Section III introduces the STBCS and discusses its properties. Section IV provides three examples of new chaotic maps generated by STBCS. Section V evaluates the performance of the three new chaotic maps and Section VI simulates them in hardware implementation. Section VII reaches a conclusion of this paper.

## II. TRADITIONAL CHAOTIC MAPS

This section reviews three existing 1-D chaotic maps as background. They will be used as seed maps to generate new chaotic maps in Section IV. To help understand this paper, we give the descriptions of important notations in Table I.

The logistic map is designed to simulate the population growth of human beings. By stretching and folding a variable within range $[0, 1]$, the logistic map can output a variable also within the range $[0, 1]$. Mathematically, the logistic map is defined as follows:

$$x_{i+1} = \mathcal{L}(x_i) = 4rx_i(1 - x_i) \tag{1}$$

where $r$ is the control parameter and $r \in [0, 1]$.

The sine map, derived from the sine function, is to transform an input angel within range $[0, \frac{1}{\pi}]$ into an output within range $[0, 1]$. By multiplying the input angel with $\pi$, the input and output of the sine map can achieve the same data range. The mathematical model of the sine map is defined by

$$x_{i+1} = \mathcal{S}(x_i) = r \sin(\pi x_i) \tag{2}$$

where the control parameter $r \in [0, 1]$.

The tent map stretches or folds the input variable according to its range. It stretches the input if the input is smaller than 0.5; otherwise, it folds the input. Its representative form can be

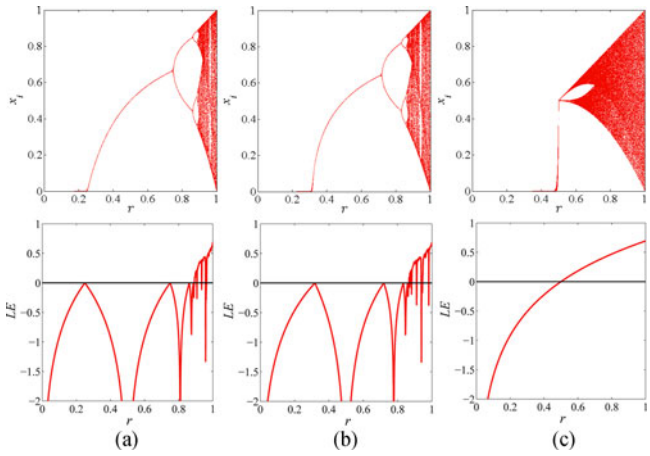


Fig. 1. Bifurcation diagrams (top row) and LEs (bottom row) of (a) the logistic map, (b) sine map, and (c) tent map.

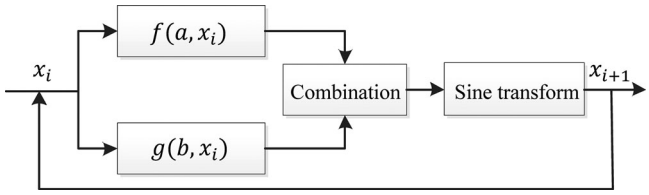


Fig. 2. Structure of STBCS.

defined as follows:

$$x_{i+1} = \mathcal{T}(x_i) = \begin{cases} 2rx_i, & \text{for} \quad x_i < 0.5 \\ 2r(1-x_i), & \text{for} \quad x_i \geq 0.5 \end{cases} \tag{3}$$

where the control parameter $r$ is also within range $[0, 1]$.

The bifurcation diagram is to describe the output ranges of a dynamical system along with its parameter's change. The Lyapunov exponent (LE) is a widely used indictor of chaotic system and a positive LE demonstrates the existence of chaotic behavior [43]. Fig. 1 plots the bifurcation diagrams and LEs of the logistic, sine, and tent maps with the change of their parameters. As can be observed, the logistic, sine, and tent maps have chaotic behaviors when $r \in [0.89, 1]$, $r \in [0.87, 1]$, and $r \in (0.5, 1)$, respectively. Even the logistic and sine maps are two different maps with totally different definitions, they have similar behaviors, which can be seen from their bifurcation diagrams and LEs. Moreover, the logistic and sine maps do not have robust chaos as periodic windows exist in their chaotic ranges, but the tent map has robust chaos when its control parameter $r \in (0.5, 1)$.

## III. Sine-Transform-Based Chaotic System

This section proposes the STBCS, discusses its properties, and analyzes its chaotic behavior.

### A. Structure of STBCS

Fig. 2 shows the structure of STBCS, where $f(a, x_i)$ and $g(b, x_i)$ are two seed maps with control parameters $a$ and $b$,

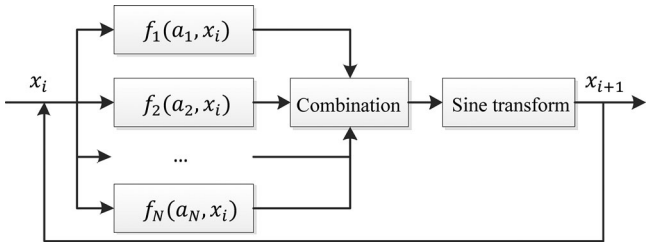


Fig. 3. Structure of extended STBCS with $N$ seed maps.

respectively. The combination is to linearly combine the outputs of the two seed maps while the sine transform performs a nonlinearly transformation to the combination results.

Mathematically, the proposed STBCS can be defined as follows:

$$x_{i+1} = \mathcal{N}(x_i) = \sin(\pi(f(a, x_i) + g(b, x_i))). \tag{4}$$

In each iteration, the input $x_i$ is simultaneously fed into $f(a, x_i)$ and $g(b, x_i)$, and then the sine transform is performed to the combination of $f(a, x_i)$ and $g(b, x_i)$'s outputs.

Any existing 1-D chaotic maps can be used as the seed maps of STBCS. Users can set the seed maps $f(a, x_i)$ and $g(b, x_i)$ as the same or different chaotic maps.

1) When $f(a, x_i)$ and $g(b, x_i)$ are the same 1-D chaotic maps, STBCS can be represented as follows:

$$x_{i+1} = \sin(\pi(f(a, x_i) + f(b, x_i))) \quad \text{or}$$
$$x_{i+1} = \sin(\pi(g(a, x_i) + g(b, x_i))). \tag{5}$$

In this case, STBCS is degraded as that the outputs of a chaotic map with two different control parameters are linearly combined and nonlinearly transformed to obtain more complex chaotic behavior.

2) When $f(a, x_i)$ and $g(b, x_i)$ are selected as two different 1-D chaotic maps, STBCS defined in (4) has the property of commutativity. Exchanging the positions of its two seed maps $f(a, x_i)$ and $g(b, x_i)$, STBCS generates an identical chaotic map.

STBCS offers users the great flexibility to generate a large number of new chaotic maps using different settings of $f(a, x_i)$ and $g(b, x_i)$. Compared with their corresponding seed maps, these generated new chaotic maps are completely different, and always have much more complex chaotic behaviors.

Moreover, the structure of STBCS in Fig. 2 can be further extended into three or more seed maps. Fig. 3 shows an extension example of STBCS with $N$ seed maps. In each iteration, the input $x_i$ is simultaneously fed into the $N$ seed maps, i.e., $f_1(a_1, x_i)$, $f_2(a_2, x_i)$, ..., and $f_N(a_N, x_i)$, and the sine transform is performed to the combination of all the seed maps' outputs. This offers users even more flexibility of selecting seed maps. The generated chaotic maps have much more complicated chaotic behaviors and more parameter settings, and thus they may have much better chaos performance and can generate more random and unpredictable output sequences. On the other hand, utilizing more seed maps may result in many negative

impacts, such as time delay, difficulty in implementation, and complexity of property analysis.

### B. Chaotic Behavior Analysis

As the chaotic behavior is a kind of observed phenomena, researchers have different opinions about its existence. Among all the chaotic behavior determining methods, the LE is one of the most significant and widely accepted indictor [43]. For the two trajectories of an identical chaotic system with slightly different initial states, LE is to measure their average exponential divergence. For a differentiable first-order difference equation $x_{i+1} = f(x_i)$, its LE can be defined by

$$\lambda_{f(x)} = \lim_{n\to\infty}\left\{\frac{1}{n}\sum_{i=0}^{n-1}\ln|f'(x_i)|\right\}. \tag{6}$$

A positive LE denotes that the two trajectories of a dynamical system with slightly different initial states exponentially diverge in each unit time and they will be totally different as system evolves, identifying chaotic behavior; while a negative LE means that their distance reduces and they will finally overlap as time goes to infinity, identifying periodic behavior. Thus, a dynamical system $x_{i+1} = f(x_i)$ is regarded as owing chaotic behavior if $\lambda_{f(x)} > 0$.

When analyzing the chaotic behavior of STBCS in (4), we first use an intermediate equation to denote the combination of two seed maps, namely $\mathcal{H}(x_i) = f(a, x_i) + g(b, x_i)$. Then, the definition of STBCS can be rewritten as follows:

$$x_{i+1} = \mathcal{N}(x_i) = \sin(\pi\mathcal{H}(x_i)). \tag{7}$$

As can be seen from the mathematical equation of the sine map in (2), we can regard (7) as a sine map, whose control parameter $r = 1$ and input is the output of $\mathcal{H}(x_i)$. We use the symbol $\tilde{\mathcal{S}}(x)$ to represent the sine map with parameter $r = 1$. Then, (7) can be rewritten as follows:

$$x_{i+1} = \mathcal{N}(x_i) = \tilde{\mathcal{S}}(\mathcal{H}(x_i)). \tag{8}$$

On the basis of the definition of LE in (6), we can get the LE of STBCS as follows:

$$\begin{aligned}\lambda_{\mathcal{N}(x)} &= \lim_{n\to\infty}\left\{\frac{1}{n}\sum_{i=0}^{n-1}\ln\left|(\tilde{\mathcal{S}}(\mathcal{H}(x_i)))'\right|\right\}\\ &= \lim_{n\to\infty}\left\{\frac{1}{n}\sum_{i=0}^{n-1}\ln\left|\tilde{\mathcal{S}}'(\mathcal{H}(x_i))\mathcal{H}'(x_i)\right|\right\}\\ &= \lim_{n\to\infty}\left\{\frac{1}{n}\sum_{i=0}^{n-1}\ln\left|\tilde{\mathcal{S}}'(\mathcal{H}(x_i))\right|\right\}\\ &\quad+\lim_{n\to\infty}\left\{\frac{1}{n}\sum_{i=0}^{n-1}\ln|\mathcal{H}'(x_i)|\right\}\\ &= \lambda_{\tilde{\mathcal{S}}(x)} + \lambda_{\mathcal{H}(x)}.\end{aligned} \tag{9}$$

Because $\tilde{\mathcal{S}}(x)$ is the sine map with parameter $r = 1$. As can be observed from Fig. 1(b) that when $r = 1$, the sine map has chaotic behavior. Thus, $\lambda_{\tilde{\mathcal{S}}(x)} > 0$. Then, the LE of STBCS can be analyzed from the following ways.

1) When $\lambda_{\mathcal{H}(x)} > 0$, namely, the first-order equation $\mathcal{H}(x)$ has chaotic behavior, $\lambda_{\mathcal{N}(x)} > 0$ and $\lambda_{\mathcal{N}(x)} > \max\{\lambda_{\tilde{\mathcal{S}}(x)}, \lambda_{\mathcal{H}(x)}\}$. This means that STBCS is chaotic and has better performance than $\tilde{\mathcal{S}}(x)$ and $\mathcal{H}(x)$.
2) When $-\lambda_{\tilde{\mathcal{S}}(x)} < \lambda_{\mathcal{H}(x)} < 0$, $\lambda_{\mathcal{N}(x)} = \lambda_{\tilde{\mathcal{S}}(x)} + \lambda_{\mathcal{H}(x)} > 0$. In this case, STBCS also has chaotic behavior.
3) When $\lambda_{\mathcal{H}(x)} < -\lambda_{\tilde{\mathcal{S}}(x)}$, $\lambda_{\mathcal{N}(x)} = \lambda_{\tilde{\mathcal{S}}(x)} + \lambda_{\mathcal{H}(x)} < 0$. In this case, STBCS does not have chaotic behavior.

In summary, if the first-order equation $\mathcal{H}(x)$ is chaotic, STBCS is always chaotic and it has better chaos performance than $\mathcal{H}(x)$ and the sine map with parameter $r = 1$; if $\mathcal{H}(x)$ is not chaotic, STBCS also has the change of owning chaotic behavior. Note that the robustness of STBCS's chaotic behavior cannot be analyzed directly, because STBCS is a general framework and the analysis of robust chaotic behavior usually applies to the chaotic maps with specific expressions [36].

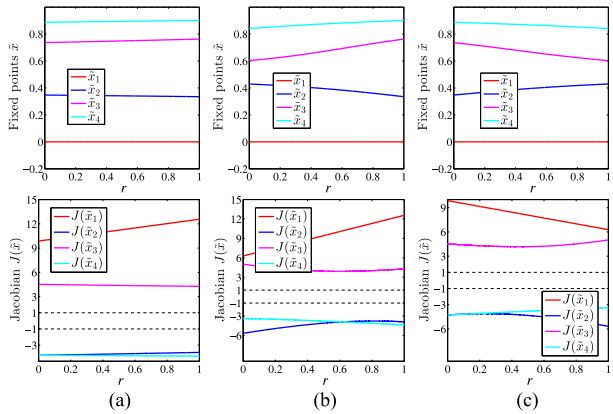


Fig. 4. Dynamics properties of the three new chaotic maps. The top and bottom rows plot the equilibrium points and their corresponding Jacobian matrix values of the (a) LS map, (b) LT map, and (c) TS map, respectively.

## IV. Examples of New Chaotic Maps

Using the proposed STBCS, users have the great flexibility to set different 1-D chaotic maps as the seed maps $f(a, x_i)$ and $g(b, x_i)$ to generate a large number of new chaotic maps. Different settings of existing maps and control parameters can obtain new chaotic maps with different chaotic behaviors. To show the effectiveness of STBCS, this section generates three examples of new chaotic maps using the three existing 1-D chaotic maps presented in Section II. For simplicity, we set control parameters $a$ as $r$ and $b$ as $1 - r$ in this paper. Users are flexible to set them in a different way.

### A. Logistic–Sine Map

***1) Definition:*** A new chaotic map called logistic–sine (LS) map can be generated when choosing the seed maps $f(a, x_i)$ as the logistic map and $g(b, x_i)$ as the sine map, and setting their control parameters $a$ as $r$ and $b$ as $1 - r$, respectively. The

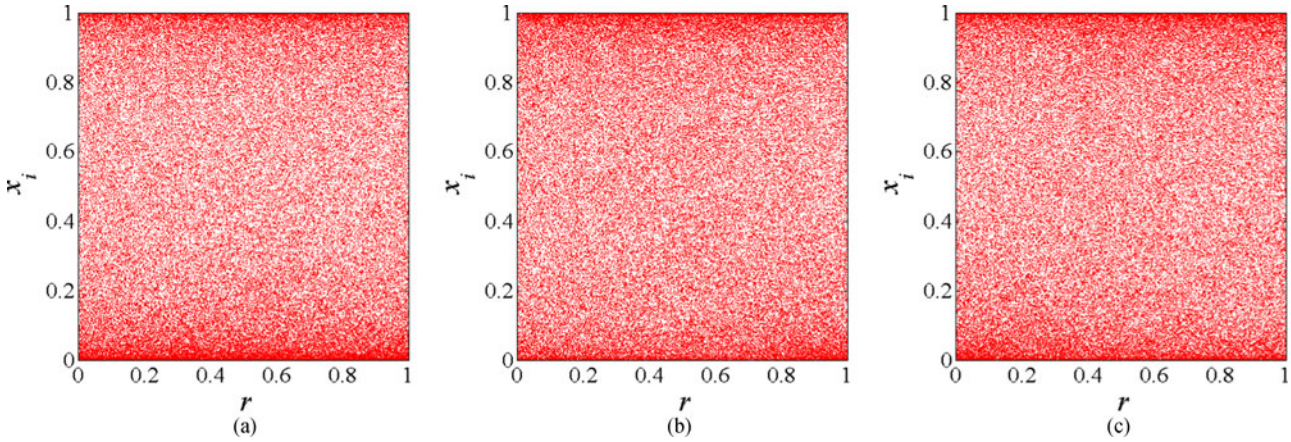


Fig. 5. Bifurcation diagrams of the (a) LS map, (b) LT map, and (c) TS map.

obtained LS map can be defined by

$$\begin{aligned} x_{i+1} &= \sin(\pi(\mathcal{L}(r, x_i) + \mathcal{S}(1-r, x_i))) \\ &= \sin(\pi(4rx_i(1-x_i) + (1-r)\sin(\pi x_i))) \end{aligned} \tag{10}$$

where the control parameter $r \in [0, 1]$.

***2) Equilibrium Point and Stability:*** Equilibrium point is an element of system's domain that maps to itself. For a dynamical system $x_{i+1} = f(x_i)$, its equilibrium points are the intersections between its curve and the 45° line, i.e., the solutions of $x_{i+1} = x_i$. Then, the equilibrium points of the LS map are the roots of the equation

$$\tilde{x} = \sin(\pi(4r\tilde{x}(1-\tilde{x}) + (1-r)\sin(\pi\tilde{x}))). \tag{11}$$

Obviously, $\tilde{x}_1 = 0$ is one equilibrium point of the LS map. Solving (11), we can find out that the LS map has a total number of four equilibrium points when its control parameter $p$ is within the range $[0, 1]$. The equilibrium point of a chaotic system owns two states: Stable state and unstable state. Its stability is associated with the slope of the system's curve at that point. When the slope falls into range $(-1, 1)$, the equilibrium point is stable and all the neighboring states will be attracted by the point; otherwise, the equilibrium point is unstable and all the neighboring states will escape from it. The slope can be calculated by the Jacobian matrix and the LS map has the Jacobian matrix as follows:

$$\begin{aligned} \mathbf{J} &= \frac{d_{\sin(\pi(\mathcal{L}(r,x_i)+\mathcal{S}(1-r,x_i)))}}{d_{x_i}} \\ &= \cos(\pi(4rx_i(1-x_i) + (1-r)\sin(\pi x_i)))\pi(4r(1 \\ &\quad - 2x_i) + (1-r)\cos(\pi x_i)\pi). \end{aligned} \tag{12}$$

The first column of Fig. 4 shows the four equilibrium points of the LS map and their corresponding Jacobian matrix values. As can be seen from the figure, the Jacobian matrix values of the four equilibrium points are all without range $(-1, 1)$ in the whole parameter settings, which means that the four equilibrium points of the LS map are always unstable. Fig. 5(a) shows the bifurcation diagram of the LS map with the change of its control parameter $r$. One can see that the LS map has outputs randomly distributed in all the parameter range. This is completely consistent with the stability of its equilibrium points, and indicates that the LS map has robust chaotic behavior in the whole parameter range.

## B. Logistic–Tent Map

***1) Definition:*** When changing the settings of one seed map in the generation procedure of the LS map, namely, setting $f(a, x_i)$ as the logistic map $\mathcal{L}(x)$, the parameters $a$ as $r$ and $b$ as $1-r$, but changing $g(b, x_i)$ as the tent map $\mathcal{T}(x)$, a new chaotic map called the logistic–tent (LT) map can be generated. The mathematical equation of the LT map is defined by

$$\begin{aligned} x_{i+1} &= \sin(\pi(\mathcal{L}(r, x_i) + \mathcal{T}(1-r, x_i))) \\ &= \begin{cases} \sin(\pi(4rx_i(1-x_i) + 2(1-r)x_i)), & \text{for } x_n < 0.5 \\ \sin(\pi(4rx_i(1-x_i) + 2(1-r)(1-x_i))), & \text{for } x_n \geq 0.5 \end{cases} \end{aligned} \tag{13}$$

where $r \in [0, 1]$ is the control parameter.

***2) Equilibrium Point and Stability:*** To find out the equilibrium points of the LT map, we set $x_{i+1} = x_i$. The equilibrium points of the LT map are the roots of the equation

$$\tilde{x} = \sin(\pi(4r\tilde{x}(1-\tilde{x}) + 2(1-r)\min\{\tilde{x}, 1-\tilde{x}\})). \tag{14}$$

By solving (14), we can find out that the LT map has four equilibrium points. The Jacobian matrix of the LT map is given by

$$\begin{aligned} \mathbf{J} &= \frac{d_{\sin(\pi(\mathcal{L}(r,x_i)+\mathcal{T}(1-r,x_i)))}}{d_{x_i}} \\ &= \begin{cases} \cos(\pi(4rx_i(1-x_i) + 2(1-r)x_i))\pi(4r(1-2x_i) \\ \quad +2(1-r)), & \text{for} \quad x_i < 0.5 \\ \cos(\pi(4rx_i(1-x_i) + 2(1-r)(1-x_i)))\pi(4r(1 \\ \quad -2x_i) - 2(1-r)), & \text{for} \quad x_i \geq 0.5. \end{cases} \end{aligned} \tag{15}$$

The four equilibrium points of the LT map and their corresponding Jacobian matrix values are plotted in the second column of Fig. 4. All the Jacobian matrix values of the four

equilibrium points are without range $(-1, 1)$. This means that the four equilibrium points of the LT map are all unstable in the whole parameter settings. As the 1-D piecewise-smooth maps can be proved to have robust chaos in an interval if they do not have stable equilibrium points in that range [36], the LT map has robust chaotic behavior in the whole parameter range. Fig. 5(b) shows the bifurcation diagram of the LT map with the change of its control parameter $r$. The outputs randomly distribute in the whole data range in all the parameter settings, which means that the LT map has complex chaotic behavior.

### C. Tent–Sine Map

***1) Definition:*** When selecting the seed maps $f(a, x_i)$ and $g(b, x_i)$ as the tent map $\mathcal{T}(x)$ and sine map $\mathcal{S}(x)$, and setting the parameters $a$ as $r$ and $b$ as $1 - r$, a new chaotic map, the tent–sine (TS) map can be generated and it is defined as follows:

$$x_{i+1} = \sin(\pi(\mathcal{T}(r, x_i) + \mathcal{S}(1 - r, x_i))) = \begin{cases} \sin(\pi(2rx_i + (1 - r)\sin(\pi x_i))) & \text{for} \quad x_n < 0.5 \\ \sin(\pi(2r(1 - x_i) + (1 - r)\sin(\pi x_i))) & \text{for} \quad x_n \geq 0.5 \end{cases} \tag{16}$$

where $r \in [0, 1]$ is a parameter.

***2) Equilibrium Point and Stability:*** The equilibrium points of the TS map are the roots of the following equation:

$$\tilde{x} = \sin(\pi(2r \min\{\tilde{x}, 1 - \tilde{x}\} + (1 - r)\sin(\pi\tilde{x}))). \tag{17}$$

Solving (17), we can find out that the TS map also has four equilibrium points. The Jacobian matrix of the TS map is given by

$$\mathbf{J} = \frac{d_{\sin(\pi(\mathcal{T}(r,x_i)+\mathcal{S}(1-r,x_i)))}}{d_{x_i}} = \begin{cases} \cos(\pi(2rx_i + (1 - r)\sin(\pi x_i)))\pi(2r \\ \quad +(1 - r)\cos(\pi x_i)\pi), & \text{for} \quad x_i < 0.5 \\ \cos(\pi(2r(1 - x_i) + (1 - r)\sin(\pi x_i)))\pi(-2r \\ \quad +(1 - r)\cos(\pi x_i)\pi), & \text{for} \quad x_i \geq 0.5. \end{cases} \tag{18}$$

The third column of Fig. 4 plots the four equilibrium points of the TS map with their related Jacobian matrix values. One can observe that all the four equilibrium points are unstable, indicating that the TS map has robust chaos in the whole parameter range. Fig. 5(c) shows the bifurcation diagram of the TS map with the change of its control parameter $r$. The TS map has chaotic behavior in the whole parameter range and its outputs also randomly distribute in the whole data range.

## V. Performance Evaluations and Comparisons

The proposed STBCS can generate new chaotic maps with better chaos performance. To demonstrate this property of STBCS, this section evaluates the three new chaotic maps generated by STBCS, and compares these chaotic maps with their corresponding seed maps and chaotic maps generated by two other generation methods, namely DPCCS [41] and ZBC [42]. To give a fair comparison environment, the parameters of chaotic maps generated by ZBC are normalized into $[0, 1]$. The comparisons are performed from the following three aspects: LE, Sample entropy (SE) [44], and Kolmogorov entropy (KE) [45].

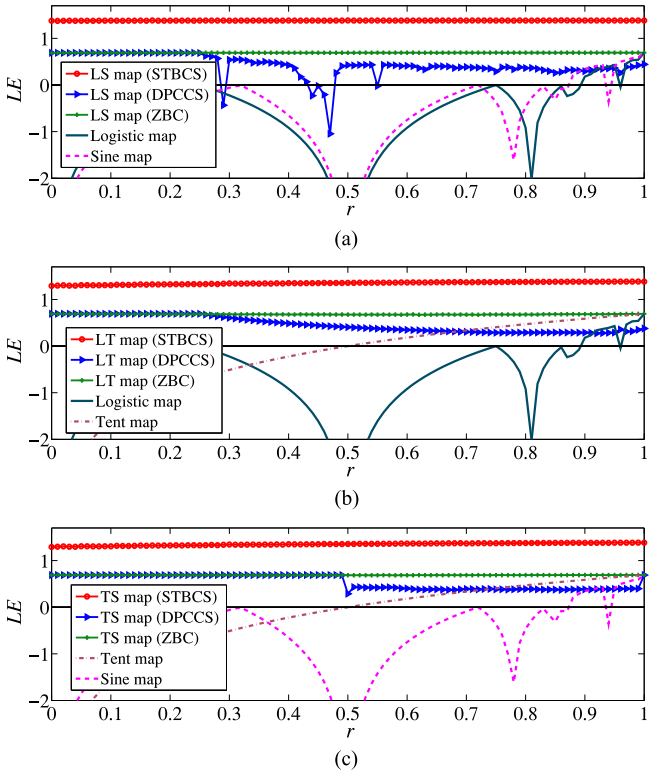


Fig. 6. LE comparisons of (a) the LS maps generated by STBCS, DPCCS, ZBC, and the corresponding seed maps, (b) the LT maps generated by STBCS, DPCCS, ZBC, and the corresponding seed maps, and (c) the TS maps generated by STBCS, DPCCS, ZBC, and the corresponding seed maps.

### A. Lyapunov Exponent

As mentioned in Section III-B that LE is a widely used indictor to identify the existence of chaotic behavior. A positive LE means that slightly different initial states of an identical equation can eventually result in totally different behaviors. So, a dynamical system with a positive LE is considered to have chaotic behavior and bigger positive LE denotes better performance. Fig. 6 shows the LE comparisons among new chaotic maps generated by different generation methods and the corresponding seed maps. One can see that in each comparison, the two seed maps only have positive LEs in few parameter settings, and the new chaotic maps generated by the proposed STBCS, DPCCS, and ZBC have positive LEs in much larger parameter ranges. Specifically, the LS map (STBCS), LT map (STBCS), TS map (STBCS), LT map (DPCCS), TS map (DPCCS), LS map (ZBC), LT map (ZBC), and TS map (ZBC) have positive

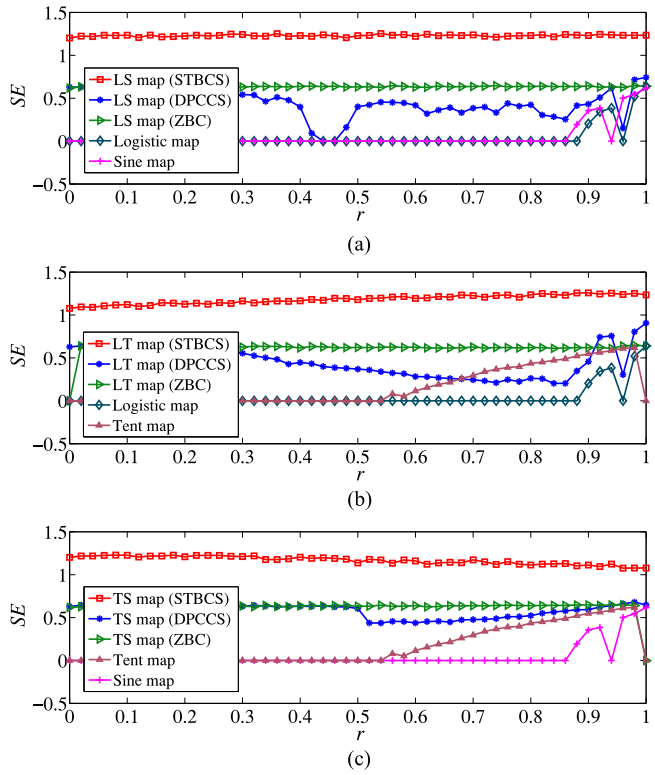


Fig. 7. SE comparisons of (a) the LS maps generated by STBCS, DPCCS, ZBC, and the corresponding seed maps, (b) the LT maps generated by STBCS, DPCCS, ZBC, and the corresponding seed maps, and (c) the TS maps generated by STBCS, DPCCS, ZBC, and the corresponding seed maps.

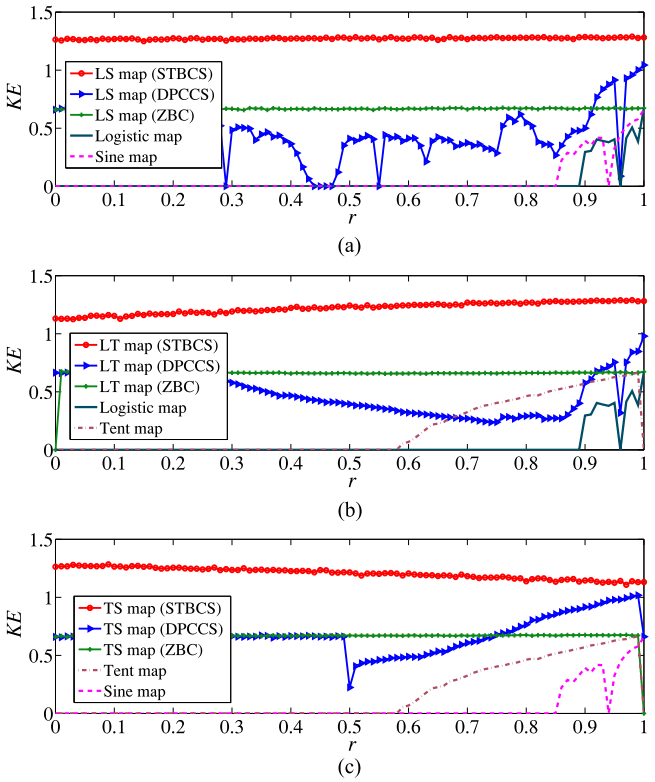


Fig. 8. KE comparisons of (a) the LS maps generated by STBCS, DPCCS, ZBC, and the corresponding seed maps, (b) the LT maps generated by STBCS, DPCCS, ZBC, and the corresponding seed maps, and (c) the TS maps generated by STBCS, DPCCS, ZBC, and the corresponding seed maps.

LEs in all the parameter settings. This means that these chaotic maps can achieve chaotic behaviors in the whole parameter ranges, indicating that they have robust chaos. Moreover, the three chaotic maps generated by STBCS have much larger LEs than chaotic maps generated by DPCCS, ZBC, and their corresponding seed maps. As a result, using the same seed maps, the proposed STBCS can generate new chaotic maps with more complex behaviors than DPCCS and ZBC.

### B. Sample Entropy

The SE is derived from the approximate entropy, which is a measure of complexity of a time series [44]. It can be used to describe the similarity of sequences generated by dynamical systems. A bigger SE reflects a lower degree of regularity, i.e., the higher complexity of dynamical system.

The SE comparisons between new chaotic maps generated by different generation methods with their corresponding seed maps are shown in Fig. 7. One can observe that all the new chaotic maps generated by STBCS, DPCCS, and ZBC have positive SEs in the whole/most parameter ranges, while their seed maps, the logistic, sine, and tent maps, only have positive SEs in small parameter ranges. Moreover, the LS, LT, and TS maps generated by the proposed STBCS can achieve much larger SEs than chaotic maps generated by DPCCS and ZBC. This also proves that STBCS can generate new chaotic maps with better complexity.

### C. Kolmogorov Entropy

The KE is a kind of metric entropy and it provides a mathematical explanation for the randomness of finite objects [45]. It can be used to measure how much extra information is needed to predict the $(t+1)$th output of a trajectory using its previous $t$ outputs. A positive KE means that extra information is required to predict a trajectory and bigger KE indicates more required information. Thus, a dynamical system with a positive KE is considered unpredictable and bigger KE means better unpredictability.

Fig. 8 depicts the KEs of different chaotic maps with the change of their parameters. It is obvious that the LS, LT, and TS maps generated by the proposed STBCS can obtain positive KEs in the whole parameter range and their KEs are much larger than new chaotic maps generated by two other methods and their corresponding seed maps. This means that the proposed STBCS can generate chaotic maps with better unpredictable.

## VI. Hardware Implementation

Even time delay exists in the proposed STBCS, the chaotic maps generated by STBCS can be implemented in practical

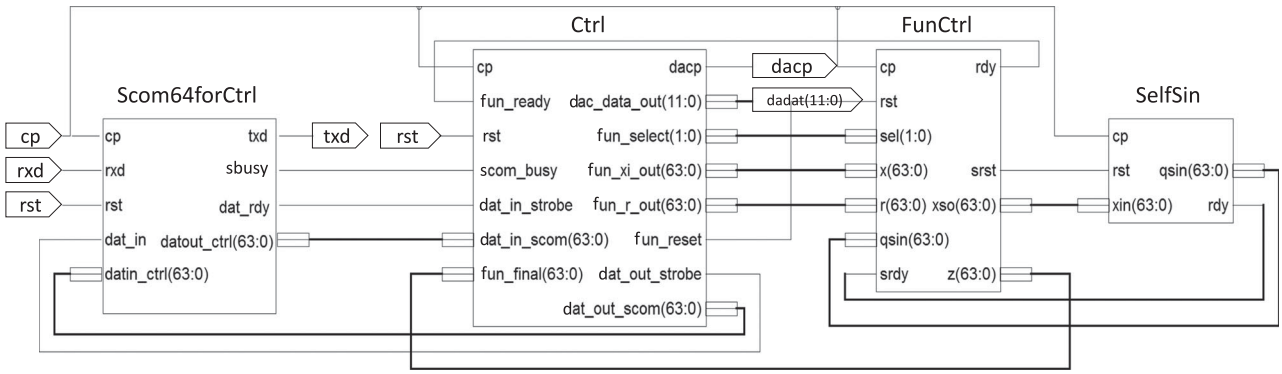


Fig. 9. FPGA structure of the three new chaotic maps generated by STBCS.

applications. To show the effectiveness of STBCS in hardware implementation, this section simulates the three newly generated chaotic maps using FPGA design.

### A. FPGA Design

As FPGA-based chaotic oscillators can achieve high frequencies, FPGA implementation is one widely used way to simulate the equations of chaotic behaviors [46]. Fig. 9 shows the structure of FPGA design for the LS, LT, and TS maps. The entire structure can be divided into four modules, including the *Scom64forCtrl*, *Ctrl*, *FunCtrl,* and *SelfSin* modules. These modules can be briefly described as follows.

1) The *Scom64forCtrl* is a communication module. The parameter *rst* is a reset key that initializes the system. The parameter *rxd* receives the initial states $(x_0, r)$ and *ref* from the computer, and returns back the iteration result to the computer through the parameter *txd*. The *ref* is a variable that decides which one of the LS, LT, and TS maps is selected to execute.
2) The *Ctrl* is a system control module. The parameter *rst* receives the data passed from the module *Scom64forCtrl* and chooses one of the LS, LT, and TS maps to execute according to the variable *ref*. It also transforms the data to and receives the iteration result from the *FunCtrl* module, and passes the received result back to the *Scom64forCtrl* module and the oscilloscope to display.
3) The *FunCtrl* is a function module that implements the LS, LT, and TS maps.
4) The *SelfSin* is also a function module that implements the sine function.

### B. Simulation Results

Here, we simulate the three new chaotic maps in MATLAB software and FPGA design. The experimental realization of FPGA design is shown in Fig. 10. The used data formats in FPGA and MATLAB designs are both the double precision of IEEE 754 standard [47]. We use the same initial states for all the simulations and set $(x_0, r) = (0.3, 0.5)$ (namely $(3FD3333333333333, 3FE0000000000000)$ in FPGA simulations). Fig. 11 plots the outputs of the three newly generated chaotic maps in FPGA and MATLAB simulations, which


Fig. 10. Experimental realization of FPGA design.

represent the hardware and software implementations, respectively. The top row plots the FPGA simulation results, while the bottom row plots the MATLAB simulation results. One can see that the outputs of software and hardware implementations are exactly the same. This means that the implementations of these new chaotic maps have consistency in different kinds of platforms. One bottleneck of chaos-based applications is that some of their used chaotic maps cannot generate the same trajectories in different platforms even with the identical initial states. These new chaotic maps can address this problem and thus can significantly promote the chaos-based applications.

## VII. Conclusion

This paper proposed the STBCS, which is a general framework of generating 1-D chaotic maps. It first combines the outputs of two existing chaotic maps, and then performs the sine transform to the combination results. Users have the great flexibility to choose any different chaotic maps as seed maps to generate a large number of new chaotic maps. We used the principle of LE to analyze the chaotic characters of STBCS and the analysis result proved its complex chaotic behavior. To demonstrate the effectiveness of STBCS in generating new chaotic maps, we provided three new chaotic maps as examples and investigated their dynamics properties. The chaos performance evaluations

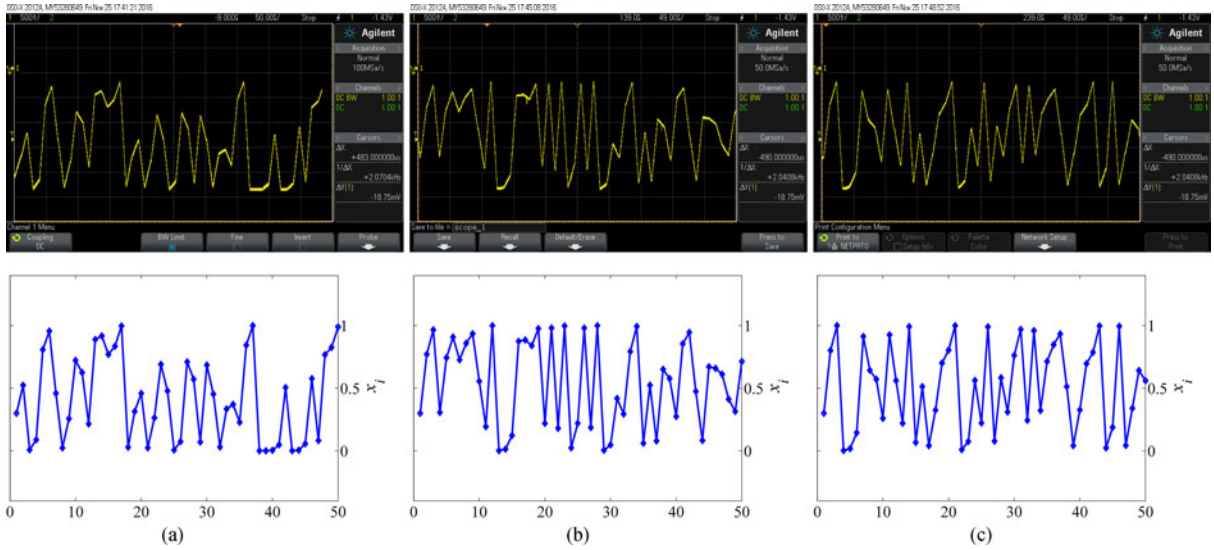


Fig. 11. Outputs of FPGA and MATLAB implementations of new chaotic maps. The top and bottom rows plot the first 50 iteration values of the (a) LS map, (b) LT map, and (c) TS map in the FPGA and MATLAB simulations, respectively. The initial states $(x_0, r)$ are set as $(0.3, 0.5)$ (namely $(3FD3333333333333, 3FE0000000000000)$ in FPGA simulations).

and comparisons using LE, SE, and KE showed that chaotic maps generated by STBCS have much larger chaotic ranges, better complexity, and unpredictability than chaotic maps generated by two other methods and their corresponding seed maps. To show the simplicity of STBCS in hardware implementation, we performed the FPGA design for the three new chaotic maps. By comparing the implementation results in hardware and software platforms, we found that these chaotic maps have the consistency in different implementation platforms.

## Acknowledgment

The authors would like to thank the anonymous reviewers for their valuable comments and suggestions that greatly contributed to improve the quality of this paper.

## References

[1] E. N. Lorenz, "Deterministic nonperiodic flow," *J. Atmos. Sci.*, vol. 20, no. 2, pp. 130–141, 1963.

[2] V. G. Ivancevic and T. T. Ivancevic, *Complex Nonlinearity: Chaos, Phase Transitions, Topology Change and Path Integrals*. Berlin, Germany: Springer, 2008.

[3] Z. Hua and Y. Zhou, "Image encryption using 2D Logistic-adjusted-Sine map," *Inf. Sci.*, vol. 339, pp. 237–253, 2016.

[4] R. L. Devaney, *An Introduction to Chaotic Dynamical Systems*, 2nd ed. Boulder, CO, USA: Westview, 2003.

[5] H. Zhao *et al.*, "Identification of nonlinear dynamic system using a novel recurrent wavelet neural network based on the pipelined architecture," *IEEE Trans. Ind. Electron.*, vol. 61, no. 8, pp. 4171–4182, Aug. 2014.

[6] H. Dimassi and A. Loria, "Adaptive unknown-input observers-based synchronization of chaotic systems for telecommunication," *IEEE Trans. Circuits Syst.—Part I, Reg. Papers*, vol. 58, no. 4, pp. 800–812, Apr. 2011.

[7] S. H. Luo and Y. D. Song, "Chaos analysis-based adaptive backstepping control of the microelectromechanical resonators with constrained output and uncertain time delay," *IEEE Trans. Ind. Electron.*, vol. 63, no. 10, pp. 6217–6225, Oct. 2016.

[8] H. Li, Y. Liu, J. Lü, T. Zheng, and X. Yu, "Suppressing EMI in power converters via chaotic SPWM control based on spectrum analysis approach," *IEEE Trans. Ind. Electron.*, vol. 61, no. 11, pp. 6128–6137, Nov. 2014.

[9] K. Cho and T. Miyano, "Chaotic cryptography using augmented Lorenz equations aided by quantum key distribution," *IEEE Trans. Circuits Syst.—Part I, Reg. Papers*, vol. 62, no. 2, pp. 478–487, Feb. 2015.

[10] H. G. Chou, C. F. Chuang, W. J. Wang, and J. C. Lin, "A fuzzy-model-based chaotic synchronization and its implementation on a secure communication system," *IEEE Trans. Inf. Forensics Security*, vol. 8, no. 12, pp. 2177–2185, Dec. 2013.

[11] R. M. May, "Simple mathematical models with very complicated dynamics," *Nature*, vol. 261, no. 5560, pp. 459–467, 1976.

[12] F. Chen, K.-W. Wong, X. Liao, and T. Xiang, "Period distribution of the generalized discrete Arnold Cat map for $N = 2^e$," *IEEE Trans. Inf. Theory*, vol. 59, no. 5, pp. 3249–3255, May 2013.

[13] C. Li, S. Li, M. Asim, J. Nunez, G. Alvarez, and G. Chen, "On the security defects of an image encryption scheme," *Image Vis. Comput.*, vol. 27, no. 9, pp. 1371–1381, 2009.

[14] C. Zhu, L. Zhang, Y. Wang, J. Liu, and L. Mao, "Periodic performance of the chaotic spread spectrum sequence on finite precision," *J. Syst. Eng. Electron.*, vol. 19, no. 4, pp. 672–678, Aug. 2008.

[15] S. Li, G. Chen, and X. Mou, "On the dynamical degradation of digital piecewise linear chaotic maps," *Int. J. Bifurcation Chaos*, vol. 15, no. 10, pp. 3119–3151, 2005.

[16] P. Bergamo, P. D'Arco, A. De Santis, and L. Kocarev, "Security of public-key cryptosystems based on Chebyshev polynomials," *IEEE Trans. Circuits Syst.—Part I, Reg. Papers*, vol. 52, no. 7, pp. 1382–1393, Jul. 2005.

[17] B. Chirikov and F. Vivaldi, "An algorithmic view of pseudochaos," *Physica D, Nonlinear Phenom.*, vol. 129, no. 3, pp. 223–235, 1999.

[18] M. Liu, S. Zhang, Z. Fan, and M. Qiu, "$H_\infty$ state estimation for discrete-time chaotic systems based on a unified model," *IEEE Trans. Syst. Man, Cybern.—Part B, Cybern.*, vol. 42, no. 4, pp. 1053–1063, Aug. 2012.

[19] A. N. Srivastava and S. Das, "Detection and prognostics on low-dimensional systems," *IEEE Trans. Syst. Man, Cybern.—Part C, Appl. Rev.*, vol. 39, no. 1, pp. 44–54, Jan. 2009.

[20] L. Lin, M. Shen, H. C. So, and C. Chang, "Convergence analysis for initial condition estimation in coupled map lattice systems," *IEEE Trans. Signal Process.*, vol. 60, no. 8, pp. 4426–4432, Aug. 2012.

[21] Z. Zhu and H. Leung, "Identification of linear systems driven by chaotic signals using nonlinear prediction," *IEEE Trans. Circuits Syst.—Part I, Fundam. Theory Appl.*, vol. 49, no. 2, pp. 170–180, Feb. 2002.

[22] X. Wu, H. Hu, and B. Zhang, "Parameter estimation only from the symbolic sequences generated by chaos system," *Chaos, Solitons & Fractals*, vol. 22, no. 2, pp. 359–366, 2004.

[23] K. Wang, W. Pei, S. Wang, Y. M. Cheung, and Z. He, "Symbolic vector dynamics approach to initial condition and control parameters estimation of coupled map lattices," *IEEE Trans. Circuits and Syst.—Part I, Reg. Papers*, vol. 55, no. 4, pp. 1116–1124, Apr. 2008.

[24] A. Skrobek, "Cryptanalysis of chaotic stream cipher," *Phys. Lett. A*, vol. 363, nos. 1/2, pp. 84–90, 2007.

[25] T. Yang, L.-B. Yang, and C.-M. Yang, "Cryptanalyzing chaotic secure communications using return maps," *Phys. Lett. A*, vol. 245, no. 6, pp. 495–510, 1998.

[26] J. Lü, X. Yu, and G. Chen, "Generating chaotic attractors with multiple merged basins of attraction: A switching piecewise-linear control approach," *IEEE Trans. Circuits Syst.—Part I, Fundam. Theory Appl.*, vol. 50, no. 2, pp. 198–207, Feb. 2003.
[27] R. Bose and S. Pathak, "A novel compression and encryption scheme using variable model arithmetic coding and coupled chaotic system," *IEEE Trans. Circuits Syst.—Part I, Reg. Papers*, vol. 53, no. 4, pp. 848–857, Apr. 2006.
[28] J. Lü and G. Chen, "A new chaotic attractor coined," *Int. J. Bifurcation Chaos*, vol. 12, no. 3, pp. 659–661, 2002.
[29] C.-Y. Li, Y.-H. Chen, T.-Y. Chang, L.-Y. Deng, and K. To, "Period extension and randomness enhancement using high-throughput reseeding-mixing PRNG," *IEEE Trans. Very Large Scale Integr. Syst.*, vol. 20, no. 2, pp. 385–389, Feb. 2012.
[30] H. Hu, Y. Xu, and Z. Zhu, "A method of improving the properties of digital chaotic system," *Chaos, Solitons & Fractals*, vol. 38, no. 2, pp. 439–446, 2008.
[31] Y. Deng, H. Hu, W. Xiong, N. N. Xiong, and L. Liu, "Analysis and design of digital chaotic systems with desirable performance via feedback control," *IEEE Trans. Syst. Man, Cybern., Syst.*, vol. 45, no. 8, pp. 1187–1200, Aug. 2015.
[32] Y. Huang, P. Zhang, and W. Zhao, "Novel grid multiwing butterfly chaotic attractors and their circuit design," *IEEE Trans. Circuits Syst.—Part II, Express Briefs*, vol. 62, no. 5, pp. 496–500, May 2015.
[33] C. Shen, S. Yu, J. Lü, and G. Chen, "Designing hyperchaotic systems with any desired number of positive Lyapunov exponents via a simple model," *IEEE Trans. Circuits Syst.—Part I, Reg. Papers*, vol. 61, no. 8, pp. 2380–2389, Aug. 2014.
[34] Y. Zhou, Z. Hua, C. M. Pun, and C. L. P. Chen, "Cascade chaotic system with applications," vol. 45, no. 9, pp. 2001–2012, Sep. 2015.
[35] S. Banerjee, J. A. Yorke, and C. Grebogi, "Robust chaos," *Phys. Rev. Lett.*, vol. 80, no. 14, pp. 3049–3052, 1998.
[36] E. Zeraoulia, *Robust Chaos and Its Applications*, vol. 79. Singapore: World Scientific, 2012.
[37] M. Drutarovsky and P. Galajda, "A robust chaos-based true random number generator embedded in reconfigurable switched-capacitor hardware," in *Proc. 17th Int. Conf. Radioelektronika*, 2007, pp. 1–6.
[38] J. Vano, J. Wildenberg, M. Anderson, J. Noel, and J. Sprott, "Chaos in low-dimensional Lotka–Volterra models of competition," *Nonlinearity*, vol. 19, no. 10, pp. 2391–2404, 2006.
[39] H.-T. Yau and J.-J. Yan, "Design of sliding mode controller for Lorenz chaotic system with nonlinear input," *Chaos, Solitons & Fractals*, vol. 19, no. 4, pp. 891–898, 2004.
[40] Y. Wu, Y. Zhou, and L. Bao, "Discrete wheel-switching chaotic system and applications," *IEEE Trans. Circuits Syst.—Part I, Reg. Papers*, vol. 61, no. 12, pp. 3469–3477, Dec. 2014.
[41] Z. Hua and Y. Zhou, "Dynamic parameter-control chaotic system," *IEEE Trans. Cybern.*, vol. 46, no. 12, pp. 3330–3341, Dec. 2016.
[42] Y. Zhou, L. Bao, and C. P. Chen, "A new 1D chaotic system for image encryption," *Signal Process.*, vol. 97, pp. 172–182, 2014.
[43] A. Wolf, J. B. Swift, H. L. Swinney, and J. A. Vastano, "Determining Lyapunov exponents from a time series," *Physica D, Nonlinear Phenom.*, vol. 16, no. 3, pp. 285–317, 1985.
[44] J. S. Richman and J. R. Moorman, "Physiological time-series analysis using approximate entropy and sample entropy," *Amer. J. Physiol.-Heart Circulatory Physiol.*, vol. 278, no. 6, pp. H2039–H2049, 2000.
[45] P. Grassberger and I. Procaccia, "Estimation of the Kolmogorov entropy from a chaotic signal," *Phys. Rev. A*, vol. 28, no. 4, pp. 2591–2593, 1983.
[46] E. Tlelo-Cuautle, J. Rangel-Magdaleno, A. Pano-Azucena, P. Obeso-Rodelo, and J. C. Nuñez-Perez, "FPGA realization of multi-scroll chaotic oscillators," *Commun. Nonlinear Sci. Numer. Simul.*, vol. 27, no. 1, pp. 66–80, 2015.
[47] *IEEE Standard for Floating-Point Arithmetic*, IEEE Standard 754-2008, 2008.

**Zhongyun Hua** (S'14–M'16) received the B.S. degree from Chongqing University, Chongqing, China, in 2011, and the M.S. and Ph.D. degrees from the University of Macau, Macau, China, in 2013 and 2016, respectively, all in software engineering.

He is currently an Assistant Professor in the School of Computer Science and Technology, Harbin Institute of Technology Shenzhen Graduate School, Shenzhen, China. His research interests include chaotic system, chaos-based applications, and multimedia security.

**Binghang Zhou** received the B.S. and M.S. degrees in control engineering from Hunan University, Changsha, China, in 1996 and 2012, respectively.

In 1996, he joined the College of Electrical and Information Engineering, Hunan University, as an Assistant Engineer, and then he has been an Engineer since 2011. His current research interests include embedded system and process control.

**Yicong Zhou** (M'07–SM'14) received the B.S. degree from Hunan University, Changsha, China in 1992, and the M.S. and Ph.D. degrees from Tufts University, Medford, MA, USA, in 2008 and 2010, respectively, all in electrical engineering.

He is currently an Associate Professor and the Director of the Vision and Image Processing Laboratory, Department of Computer and Information Science, University of Macau, Macau, China. His research interests include chaotic systems, multimedia security, image processing and understanding, and machine learning.

Dr. Zhou is a Leading Co-Chair of the Technical Committee on cognitive computing in the IEEE SYSTEMS, MAN, AND CYBERNETICS SOCIETY. He is an Associate Editor of *Neurocomputing* and the *Journal of Visual Communication and Image Representation*. He received the Third Price of the Macau Natural Science Award in 2014.